JOURNAL OF MATERIALS SCIENCE 18 (1983) 2371–2379

^{55}Fe diffusion in magnetite crystals at 500° C and its relevance to oxidation of iron

A. ATKINSON, M. L. O'DWYER, R. I. TAYLOR
Materials Development Division, Building 552, AERE Harwell, Didcot, UK

A computer controlled sputter-sectioning apparatus is described which is particularly useful for self diffusion studies at "low" temperatures (D in the range 10^{-12} to 10^{-19} cm^2 sec^{-1}). The technique has been applied to measure the diffusion coefficient of ^{55}Fe in the magnetite lattice as a function of oxygen activity at 500° C. The results are in broad agreement with an extrapolation of pre-existing high temperature diffusion data ($T > 900$° C). The low temperature data have been used to estimate the rate constant for magnetite formation on iron in CO_2 + 1 vol% CO at 500° C and this is found to be 250 times smaller than the experimentally measured value. This disagreement is probably attributable to diffusion along oxide grain boundaries during oxidation. The rate constant for the formation of magnetite during the oxidation of iron in oxygen has also been calculated from the diffusion data and is compared with the measured rate constant for temperatures between 325 and 1100° C.

1. Introduction

The oxidation of iron is an important reaction with a bearing on many technological areas and consequently much effort has been expended in trying to improve the understanding of the reaction mechanism. The work of Himmel *et al.* [1] was a milestone in this area. They made measurements of the tracer diffusion coefficients of iron in the iron oxides FeO (wüstite), Fe_3O_4 (magnetite) and Fe_2O_3 (haematite) and also of the rates of growth of these oxides in the oxidation of iron at high temperature. They found good agreement between the measured parabolic rate constant for wüstite formation (the principal oxide in the scale) and that calculated from the iron tracer diffusion data using Wagner's [2] theory of oxide scale growth.

The rate of growth of wüstite upon iron is so rapid that ferrous alloys cannot be utilized if the conditions are such that wüstite would be formed in the scale. As a result, high temperature iron-based alloys must contain large concentrations of alloying elements which will form more protective oxides in the scale (e.g. Cr_2O_3). However, wüstite is only stable at temperatures above 570° C and the scales formed on iron at temperatures below 570° C consist of only the more protective magnetite and haematite; magnetite being the principal one. Therefore, low alloy steels can be used at temperatures below 570° C, in which case they rely on magnetite for protection against rapid oxidation. Consequently, it is at these relatively low temperatures that the mechanism of growth of magnetite scales upon iron is of interest.

Atkinson and Taylor [3] have used ^{55}Fe and ^{18}O tracers and Gleave *et al.* [4] ^{18}O tracer to study the motion of species in growing magnetite scales at 500° C. These studies support the widely held belief that the rate of growth of the magnetite is controlled by the outward diffusion of iron through the scale. (Inward diffusion of oxygen was observed under certain conditions, but this is most probably via the gas phase through fissures in the oxide.) It should therefore be possible in principle to explain the rate of magnetite formation quantitatively in terms of the diffusion coefficient of iron in magnetite.

Dieckmann and Schmalzried [5, 6] have carried out a thorough study of the diffusion of ^{59}Fe in magnetite over its stability field at temperatures in the range 900 to 1400° C. Within this temperature range the tracer diffusion coefficient is described by

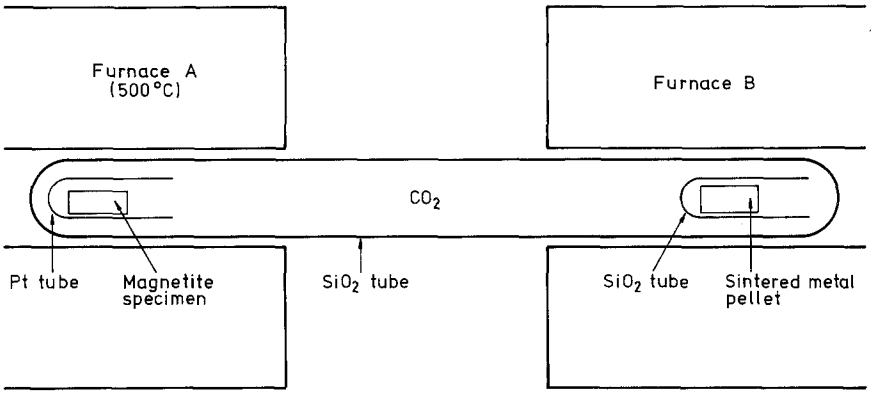

Figure 1 Schematic diagram showing the arrangement used to establish a known CO_2:CO ratio, and hence oxygen activity, at the diffusion specimen.

the expression

$$D^*_{Fe} = 4 \times 10^{-11} \exp[+1.45(eV)/kT] a_{O_2}^{2/3} + 8 \times 10^{7} \exp[-6.37(eV)/kT] a_{O_2}^{-2/3} \, cm^2 \, sec^{-1} \quad (1)$$

in which a_{O_2} is the activity of molecular oxygen. The first term in Equation 1 is from diffusion by a vacancy mechanism and dominates at "high" oxygen activity whereas the second term is from diffusion by interstitial iron ions and is dominant at low oxygen activity. Isotope effect measurements [7] are in agreement with this interpretation.

The purpose of the work described here was to measure the diffusion coefficient of iron in magnetite over its stability range at the much lower temperature of 500° C which is of interest from the point of view of the protective properties of magnetite scales on iron. The data are then used to calculate the expected rate of growth of magnetite on iron which is compared with the rate found in oxidation experiments.

2. Experimental techniques

2.1. Diffusion specimens

The magnetite diffusion specimens were provided by H. Schmalzried and have been described by Dieckmann and Schmalzried [5]. They were in the form of discs approximately 10 mm diameter by 2 mm thickness and each disc was either a single crystal or a few large crystals. The diffusion surface of each specimen was polished to a flat mirror finish using diamond abrasive and then the specimens were annealed in a flowing gas mixture of CO_2 containing 0.1 vol% CO at 900° C. This annealing treatment was to stabilize the structure of dislocations which are inevitably introduced by the mechanical surface preparation.

2.2. Diffusion anneals

The establishment of known oxygen activities at 500° C is difficult to ensure using flowing gas mixtures because the rates of equilibration in CO_2/CO or H_2O/H_2 mixtures are sluggish at these temperatures. The oxygen activities were therefore established in a closed system, which is shown in Fig. 1. The SiO_2 tube was loaded with the diffusion specimen, inside a platinum tube with one closed end, in furnace A and a pressed and sintered pellet of a metal powder in furnace B. (The metal pellet had been previously sintered in CO_2 + 0.1 vol% CO for 30 min at 700° C and then stored in a desiccator to prevent uptake of moisture.) The metals which were used are listed in Table I. The SiO_2 tube was evacuated and filled with CO_2 at a pressure of 0.4 atm at room temperature and then the tube was sealed. Furnace B was then raised to a temperature such that the metal pellet, in equilibrium with its lowest oxide, would establish the required CO_2:CO ratio in the gas phase. The temperature of the specimen was then raised to 500° C for the duration of the anneal using furnace A. This procedure was used to pre-anneal each specimen to establish the equilibrium defect structure in the near surface region at the required oxygen activity.

After the pre-diffusion anneal the SiO_2 tube was broken and the specimen removed. ^{55}Fe tracer was applied to the specimen surface by vacuum evaporation of $^{55}FeCl_3$ and then heating in air at 200° C for 10 min to convert the chloride to the oxide. The diffusion anneal proper was then carried out in the same manner as previously described for the pre-diffusion anneal. Any re-equilibration of the defect structure near the specimen surface would take place in a

TABLE I Details of diffusion anneals at 500° C

a_{O_2} (atm)	Metal and temperature of furnace B (° C)	Anneal time (sec)	D^* ($cm^2 sec^{-1}$)	Maximum penetration (μm)
7×10^{-20}	Cu, 710	1.8×10^4	3.2×10^{-15}	0.4
7×10^{-20}	Cu, 710	8.65×10^4	1.1×10^{-14}	1.0
2×10^{-20}	Cu, 760	8.64×10^4	2.1×10^{-14}	1.8
2×10^{-21}	Cu, 870	1.82×10^4	4.0×10^{-15}	0.5
1×10^{-22}	Cu, 1000	3.48×10^5	4.2×10^{-17}	1.6
1×10^{-24}	Co, 500	6.05×10^5	4.6×10^{-16}	1.0
2×10^{-25}	Co, 630	6.05×10^5	9.7×10^{-17}	0.8
1×10^{-25}	Ni, 950	6.05×10^5	4.0×10^{-16}	0.7
2×10^{-26}	Co, 800	6.05×10^5	2.1×10^{-16}	0.5
5×10^{-27}	Co, 1000	1.73×10^5	5.7×10^{-16}	0.6
1×10^{-29}	Fe, 500	1.8×10^4	3.5×10^{-15}	0.3

time which is short compared with the diffusion anneal.

2.3. Automated sectioning of diffusion specimens

In general, the measurement of tracer diffusion coefficients at relatively low temperatures requires the diffusion specimen to be sectioned on a submicron scale. A method by which this was accomplished on oxide specimens has been described in an earlier publication [8]. The principle of the method is that the specimen forms part of the cathode in a radiofrequency (RF) sputtering system in which the sputtered material is collected on the anode. An aluminium collector disc which formed part of the anode could be removed and the collected activity counted. This type of sectioning is particularly suited to automation and control by a small computer and this has now been done as described below.

The heart of the automated system is an anode assembly into which is built a magazine holder for the aluminium collector discs. The discs can be brought in sequence into the collecting position by a mechanism which is activated from outside the vacuum system. The configuration of the anode assembly (which is electrically grounded) is shown in Figs. 2 to 4. At the start of a profiling sequence, all the aluminium collector discs are in the downstack of the magazine (Fig. 2). The disc at the bottom of the downstack is in position to receive material sputtered from the sample through an aperture in the base of the anode (Fig. 3) and the magazine can be loaded with up to 40 discs. The collector discs are located in individual carriers (Fig. 4) which have bevelled edges. When the next collector disc is required to be in place over the aperture, the pneumatic actuator pushes the carrier which is at the base of the downstack across and into the upstack of the magazine. The bevelled edge of the carrier ensures that it is inserted underneath other carriers already in the upstack. When the actuator returns to its starting position all the carriers in the downstack drop and the next collector is left over the aperture in position for the next section. Situated as close as possible to the aperture is a quartz crystal film thickness transducer (Kronos type FTT-300, Torrance CA 90501, USA) which is used to measure the thickness of material removed in each section. Water cooling is provided to maintain the base of the anode and the film thickness transducer at constant temperature. The anode faceplate is detachable so that it can be replaced when the activity on it has reached an unacceptably high level.

The operation of the unit is controlled using a Commodore PET microcomputer which interfaces with the sputtering system using a MOUSE interface module (6000 Laboratory Series, Harwell, UK). As shown in Fig. 5, the computer controls the following functions; switching the RF power on and off, reading the film thickness monitor and changing the collector disc. The timing of all functions is controlled by the computer's internal clock.

3. Results and discussion

Details of the diffusion anneals are given in Table I including the type of metal which, as a sintered pellet, was used at the temperature shown (furnace B) to establish the required CO_2:CO ratio in the

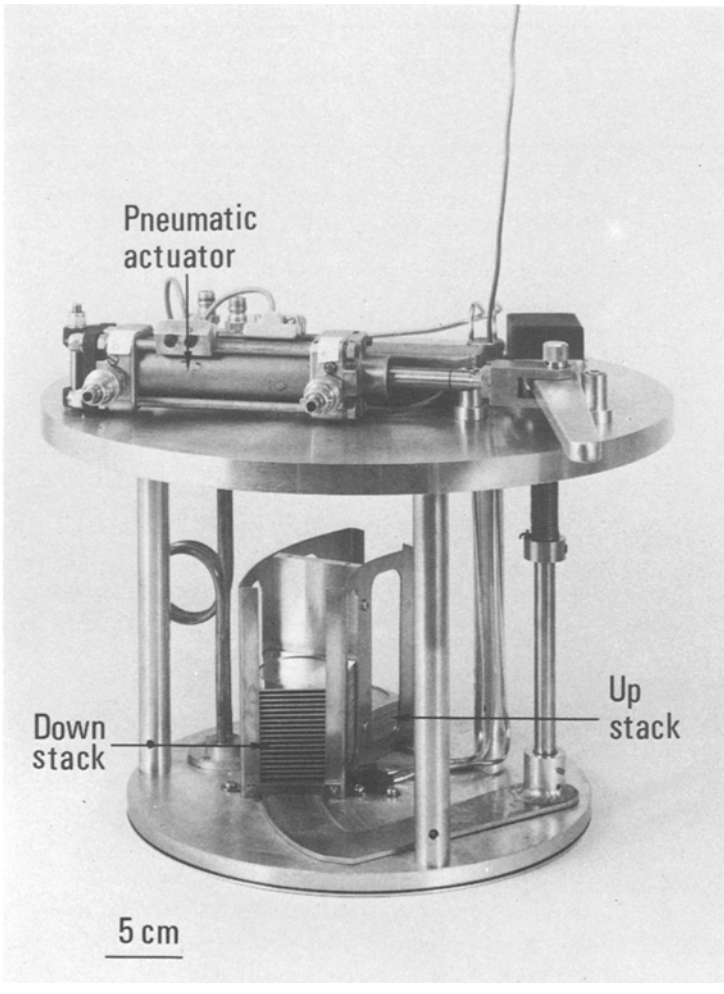

Figure 2 General view of the anode assembly showing the magazine holding the collector discs.

the closed diffusion system. The measured diffusion coefficients and the maximum depth of penetration of tracer in each experiment are also given. It can be seen that all the diffusion profiles were within 2 μm of the surface. A typical tracer penetration profile is shown in Fig. 6 in which the same data are plotted against both the penetration depth and the square of the penetration depth. Except for a region very close to the surface, the plot against the square of the penetration depth gives the better straight line. Such behaviour is usually indicative of bulk lattice diffusion. From plots of this type the diffusion coefficients were extracted using the known solution for diffusion from a thin source into a uniform medium.

The measured diffusion coefficients are plotted as a function of a_{O_2} in Fig. 7. The data show considerable scatter, similar to that observed in a previous study of diffusion in NiO at relatively low temperatures [9]. The error bars shown in Fig. 7 represent only the uncertainty in the interpretation of the diffusion profiles. This error is large in those instances where plots of the type shown in Fig. 6 showed considerable curvature, probably as a result of the influence of dislocations [10]. The variable dislocation content near the specimen surface (introduced by polishing), hold-up of tracer on the surface and the unknown precision of the method used to establish the oxygen activity are all possible sources of error which are difficult to quantify and are not included in the error bars.

The broken curve in Fig. 7 is extrapolated from the high temperature data of Dieckmann and Schmalzried using Equation 1. Despite the scatter in the measurements it is evident that the measured diffusion coefficients at 500°C are in broad agreement with the extrapolation of the high temperature data. This means that diffusion

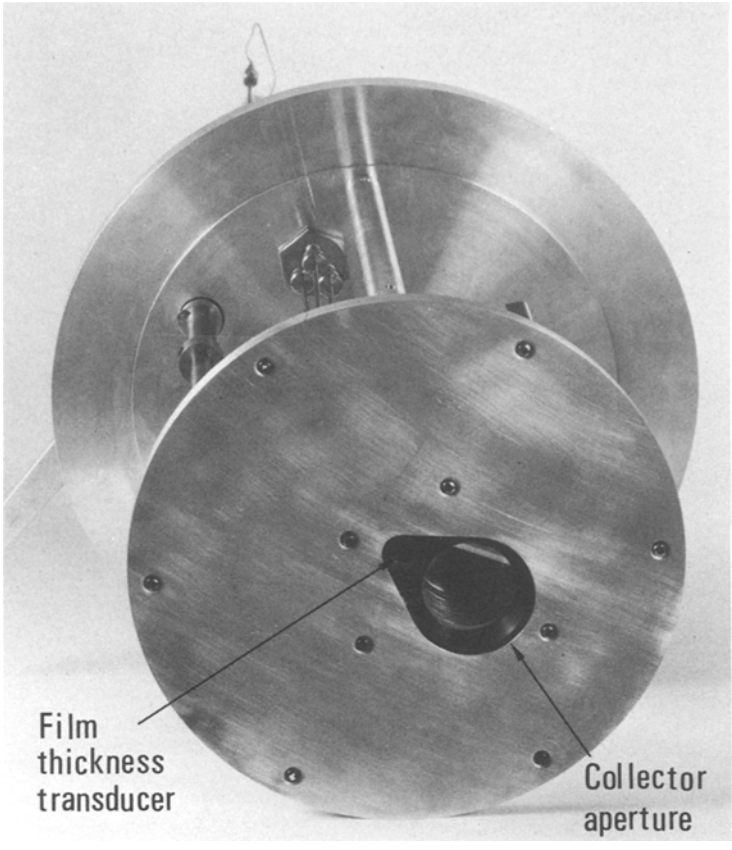

Figure 3 Underside view of the anode assembly.

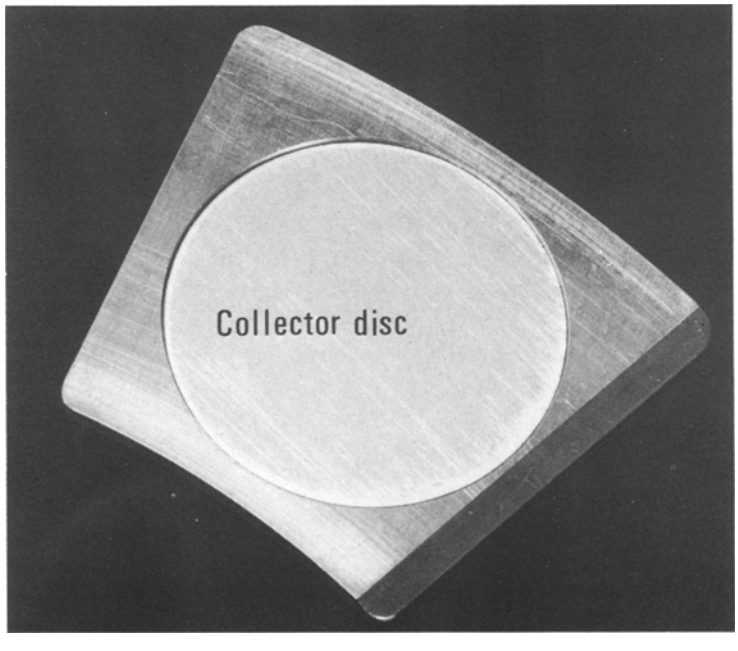

Figure 4 Aluminium collector disc located in its carrier.

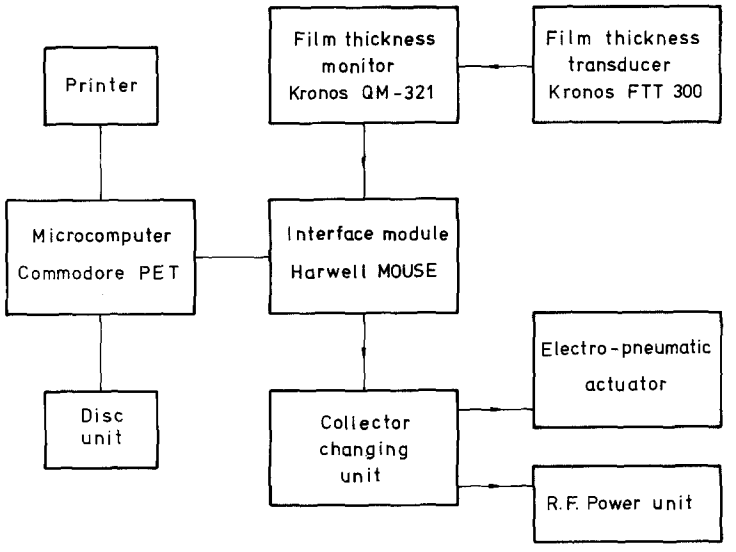

Figure 5 Block diagram of the computer control system.

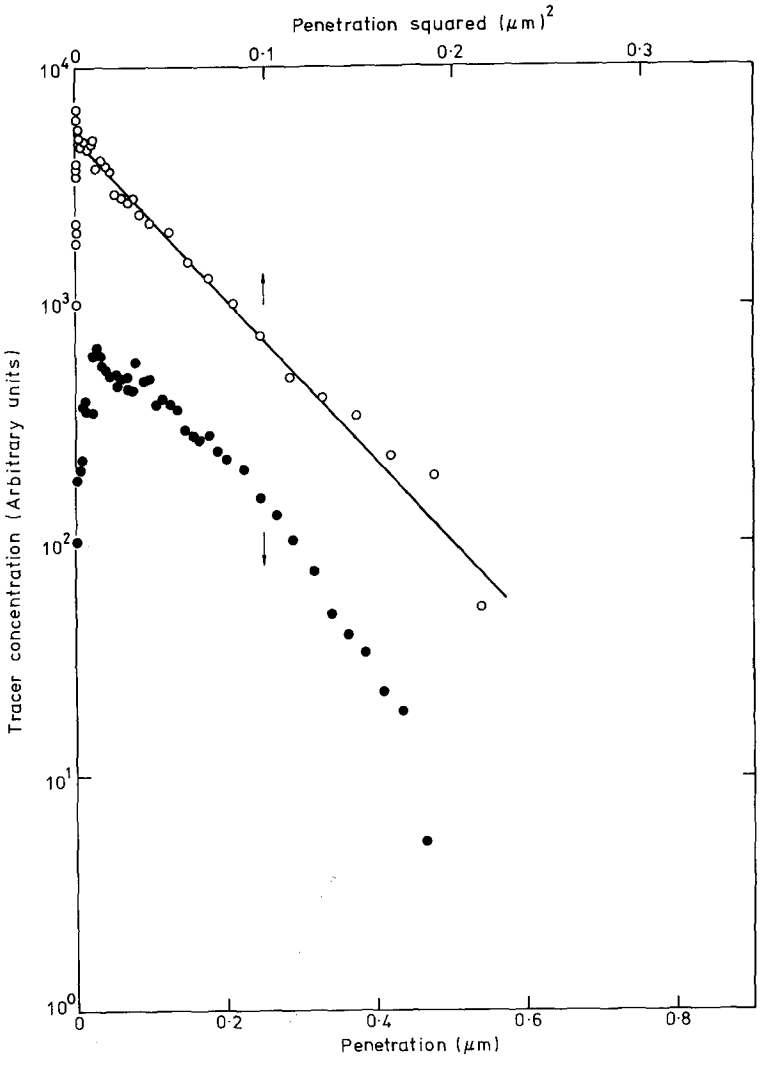

Figure 6 A typical diffusion profile for ^{55}Fe tracer diffused into magnetite for 7 days at 500°C and $a_{O_2} = 2 \times 10^{-26}$ atm. NB the different scale for the upper and lower plots.

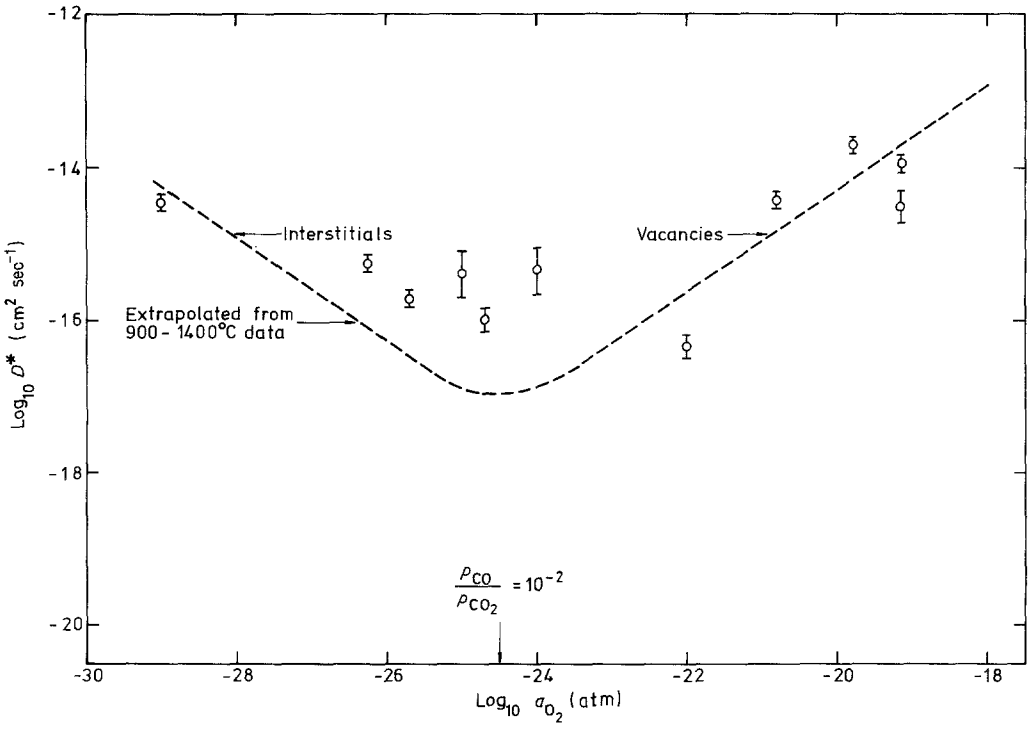

Figure 7 The diffusion coefficient of ^{55}Fe in magnetite at 500° C as a function of a_{O_2} across the magnetite phase field. The broken line is extrapolated from the high temperature data of Dieckmann and Schmalzried [5].

in these magnetite samples at 500° C has not been grossly influenced either by impurities or by any ordering phenomena on the cation sublattice. Diffusion in ionic crystals having small deviations from stoichiometry is often sensitive to small concentrations of heterovalent impurity because the requirement to neutralize the effective charge of the impurity leads to the creation or destruction of intrinsic defects. However, in magnetite this charge compensation can readily be accommodated by a small adjustment to the Fe^{3+}: Fe^{2+} ratio so that the defect structure is hardly perturbed despite the fact that magnetite is probably stoichiometric within its field of stability (e.g. magnetite is stoichiometric Fe_3O_4 at $a_{O_2} = 7 \times 10^{-8}$ atm at 1200° C [6]). The defect model favoured by Dieckmann and Schmalzried at high temperatures is one in which the occupancy of a given cation site in the spinel lattice (having octahedral or tetrahedral oxygen coordination) is unaffected by whether the ion is divalent or trivalent and that vacancies are equally likely for both types of site. These assumptions may not be valid at lower temperatures when ordering in the cation sublattice takes place. The Curie temperature of magnetite is 585° C and below this temperature the magnetic properties are consistent with the cations being ordered in the inverse spinel structure. Thus an order/disorder transformation on the cation sublattice is expected to occur between 585 and 900° C. However, Dieckmann and Schmalzried's calculations [6] indicate that the dependence of D^* on a_{O_2} is relatively insensitive to the degree of ordering amongst the cations and therefore Equation 1 will be a good approximation at low temperatures provided that the ordering energy is small in comparison with the Arrhenius energies. (This is a reasonable assumption since kT is only 0.074 eV at the Curie temperature.)

In conclusion, the broad agreement between the diffusion coefficients measured at 500° C and those extrapolated from much higher temperatures is not surprising since the effects of both impurities and ordering are expected to be small.

4. Diffusion in magnetite and the oxidaton of iron

Garnaud and Rapp [11] used Dieckmann and Schmalzried's diffusion data to calculate the expected parabolic rate constant (oxide thickness squared divided by time) for magnetite growth when formed simultaneously with wüstite during the oxidation of iron at 1100° C. The calculated

rate constant agreed with the measured value to within a factor of two. This can be regarded as sufficiently good agreement to show that the rate of magnetite growth is controlled by the outward diffusion of iron ions through the magnetite lattice at high temperature.

Application of Wagner's theory to the exclusive formation of magnetite on iron by the outward diffusion of iron ions yields the following expression for the rate constant defined as $x^2 = k_p t$:

$$k_p = \frac{4}{3} \int_{a'_{O_2}}^{a''_{O_2}} f^{-1} D^* \, d\ln a_{O_2} \qquad (2)$$

In this expression a'_{O_2} and a''_{O_2} are the activities of molecular oxygen at the inner and outer interfaces of the magnetite and f is the correlation factor for the diffusion mechanism. f is approximately 0.5 when transport occurs by a vacancy mechanism and in the range 0.4 to 1 for the likely mechanisms involving interstitials [7]. For convenience f has been taken to be 0.5 for both mechanisms. For an oxidizing atmosphere of CO_2 with 1 vol% CO at 500° C the evaluation of Equation 2 requires an integration between oxygen activities of approximately 10^{-25} to 10^{-29} atm which is on the interstitial branch of the curve in Fig. 7. When equation 2 is evaluated using the measured diffusion data (Fig. 7) for these conditions we find that k_p is estimated to be approximately 2×10^{-14} cm^2 sec^{-1}. The measured parabolic rate constant is 5×10^{-12} cm^2 sec^{-1} [12] which is 250 times faster than the calculated value.

The rate of oxidation of nickel to NiO is similarly faster than expected from known lattice diffusion coefficients and this has been shown to be due to the dominant transport mechanism, at low temperatures, being the diffusion of nickel along NiO grain boundaries [13]. It therefore seems probable that the diffusion of iron along magnetite grain boundaries is the dominant transport process in the oxidation of iron at temperatures below 570° C.

When iron is oxidized at temperatures above 570° C magnetite grows on a much thicker subscale of wüstite. Furthermore, when iron is oxidized in air the magnetite is usually overgrown with a thinner layer of haematite. Garnaud and Rapp [11] have shown that under these conditions the parabolic rate constant for the growth of the magnetite layer is approximately equal to that for magnetite formation alone under the maximum chemical potential difference allowed by the magnetite phase field. That is, it can be evaluated from Equation 2 by putting a'_{O_2} equal to the oxygen activity for the wüstite/magnetite equilibrium and a''_{O_2} to that for magnetite/haematite equilibrium. The complications due to the simultaneous growth of three layers result in only a minor correction, which can be made if the relative thicknesses of the layers are known.

This "maximum" parabolic rate constant has been calculated from the diffusion data and is shown in the Arrhenius plot in Fig. 8 together with the experimental rate constants taken from the literature and which have been corrected for multilayer growth where possible. Fig. 8 shows that the measured value tends to be greater than the predicted one for temperatures below 700° C. Such behaviour is consistent with the conclusion drawn from the similar comparison made earlier for oxidation of iron in CO_2 + 1 vol% CO at 500° C in which the measured rate constant was 250 times greater than the calculated one. The good agreement in Fig. 8 between the predicted parabolic rate constant and that measured in some studies at low temperatures [14, 15] may result from a fortuitous combination of the opposing effects of grain boundary diffusion in the oxide and deviations from the assumed chemical equilibria at the boundaries of the magnetite scale [19].

5. Conclusions

1. Sectioning of diffusion specimens by sputtering is a process which is well suited to automation under microcomputer control, thereby relieving the experimenter of many time-consuming repetitive tasks.

2. The diffusivity of iron in the magnetite lattice at 500° C is in broad agreement with diffusion data extrapolated from much higher temperatures. This is consistent with the expected insensitivity of the diffusivity to impurities and ordering on the cation sublattice.

3. The diffusion data have been used to calculate the expected parabolic rate constant for magnetite growth during the oxidation of iron. At 1100° C the calculated value is within a factor of two of the measured value, but at 500° C for the oxidation in CO_2 + 1 vol% CO the measured value is 250 times faster than calculated. This is probably due to the dominant transport process at 500° C being diffusion along oxide grain boundaries, rather than through the lattice. The measured rate constant for magnetite growth when

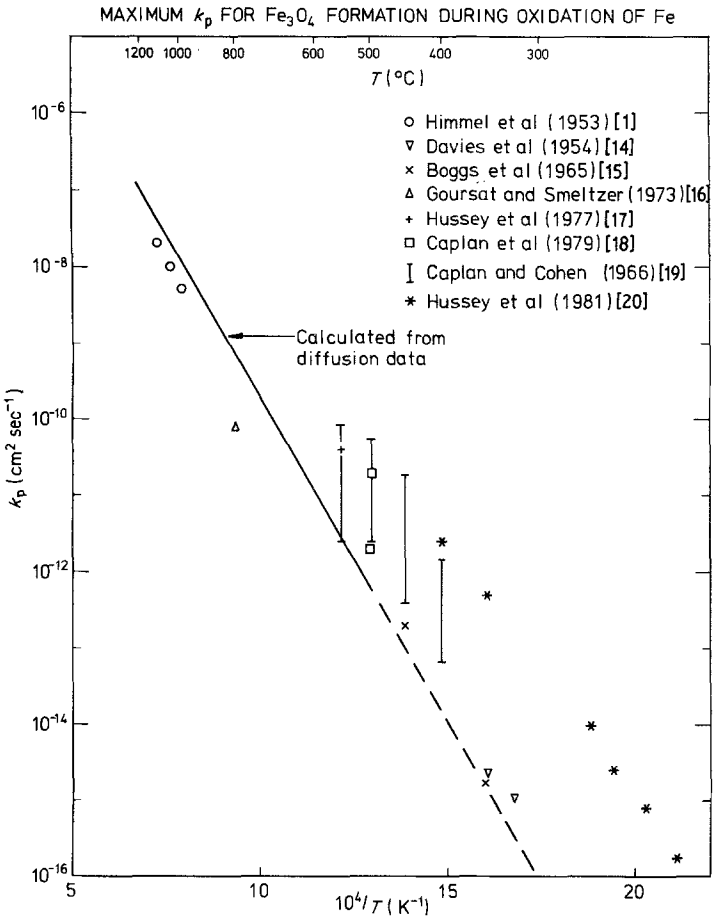

Figure 8 Arrhenius plot of the parabolic rate constant for magnetite growth during the oxidation of iron under conditions which are expected to impose, across the magnetite, the maximum chemical potential difference allowed by the magnetite stability field. Oxidation data are taken from [1, 14–20].

overgrown by a layer of haematite is similarly greater than the calculated one at temperatures below 700° C.

Acknowledgements

The authors are particularly grateful to Mr K. A. J. Gotch for his help in designing the automatic sectioning apparatus and Mr M. P. Stevens for design of the computer interface. We also wish to thank Professor H. Schmalzried for providing the magnetite diffusion specimens. This paper is published by kind permission of the United Kingdom Atomic Energy Authority. © UKAEA 1983.

References

1. L. HIMMEL, R. F. MEHL and C. E. BIRCHENALL, *Trans. AIME* **197** (1953) 827.
2. C. WAGNER, *Z. Phys. Chem.* **B21** (1933) 25.
3. A. ATKINSON and R. I. TAYLOR, UK Atomic Energy Report AERE-R10289 (1981).
4. C. GLEAVE, J. M. CALVERT, D. G. LEES and P. C. ROWLANDS, *Proc. Roy. Soc. London* **A379** (1982) 409.
5. R. DIECKMANN and H. SCHMALZRIED, *Ber. Bunsen-Ges.* **81** (1977) 344.
6. *Idem, ibid.* **81** (1977) 414.
7. N. L. PETERSON, W. K. CHEN and D. WOLF, *J. Phys. Chem. Solids* **41** (1980) 709.
8. A. ATKINSON and R. I. TAYLOR, *Thin Solid Films* **46** (1977) 291.
9. *Idem, Phil. Mag.* **A39** (1979) 581.
10. A. D. LE CLAIRE and A. RABINOVITCH, *J. Phys. C: Solid State Phys.* **15** (1982) 3455.
11. G. GARNAUD and R. A. RAPP, *Oxid. Met.* **11** (1977) 193.
12. P. T. MOSELEY, G. TAPPIN and J. C. RIVIERE, *Corros. Sci.* **22** (1982) 69.
13. A. ATKINSON, R. I. TAYLOR and A. E. HUGHES, *Phil. Mag.* **A45** (1982) 823.
14. D. E. DAVIS, U. R. EVANS and J. N. AGAR, *Proc. Roy. Soc. London* **A225** (1954) 443.
15. W. E. BOGGS, R. H. KACHIK and G. E. PELLISSIER, *J. Electrochem. Soc.* **112** (1965) 539.
16. A. G. GOURSAT and W. W. SMELTZER, *Oxid. Met.* **6** (1973) 101.
17. R. J. HUSSEY, G. I. SPROULE, D. CAPLAN and M. J. GRAHAM, *Oxid. Met.* **11** (1977) 65.
18. D. CAPLAN, G. I. SPROULE, R. J. HUSSEY and M. J. GRAHAM, *ibid.* **12** (1978) 67.
19. D. CAPLAN and M. COHEN, *Corros. Sci.* **6** (1966) 321.
20. R. J. HUSSEY, D. CAPLAN and M. J. GRAHAM, *Oxid. Met.* **15** (1981) 421.

Received 2 November
and accepted 20 December 1982